Unimolecular dynamics from kinetic energy release distributions. V. How does the efficiency of phase space sampling vary with internal energy?

A. Hoxha, R. Locht, A. J. Lorquet, J. C. Lorquet, and B. Leyh[a)]
Département de Chimie, B6c, Université de Liège, Sart-Tilman, B-4000 Liège 1, Belgium

(Received 19 July 1999; accepted 1 September 1999)

A retarding field technique coupled with a quadrupole mass analyzer has been used to obtain the kinetic energy release distributions (KERDs) for the $C_2H_3Br^+ \rightarrow [C_2H_3]^+ + Br$ dissociation as a function of internal energy. The KERDs obtained by dissociative photoionization using the He(I), Ne(I), and Ar(II) resonance lines were analyzed by the maximum entropy method and were found to be well described by introducing a single dynamical constraint, namely the relative translational momentum of the fragments. *Ab initio* calculations reveal the highly fluxional character of the $C_2H_3^+$ ion. As the energy increases, several vibrational modes are converted in turn into large-amplitude motions. Our main result is that, upon increasing internal energy, the fraction of phase space sampled by the pair of dissociating fragments is shown to first decrease, pass through a shallow minimum around 75%, and then increase again, reaching almost 100% at high internal energies (8 eV). This behavior at high internal energies is interpreted as resulting from the conjugated effect of intramolecular vibrational redistribution (IVR) and radiationless transitions among potential energy surfaces. Our findings are consistent with the coincidence data of Miller and Baer, reanalyzed here, and with the KERD of the metastable dissociation. © *1999 American Institute of Physics.* [S0021-9606(99)01644-X]

I. INTRODUCTION

Statistical theories of mass spectra assume that the internal energy of an ionized molecule is completely randomized among all available degrees of freedom before the dissociation takes place. One of the basic present questions in reaction dynamics is how far this ergodic hypothesis holds. The distributions of kinetic energy released during the fragmentation process (KERDs) contain information about the reaction dynamics[1–10] and provide a complementary and more severe test for the validity of the statistical theories of mass spectra than the measurement of the unimolecular reaction rate constants.[11]

The maximum entropy method[12–15] has seldom been used for the analysis of the KERD data of ionic systems, mainly in the form of a surprisal analysis.[5,16–22] Only recently have detailed maximum entropy analyses of KERDs of ionic systems been reported.[23–25]

The maximum entropy theory is based on the Bayesian approach of probability. It compares the observed KERD with a reference state called the prior distribution defined as the distribution one can assume without having any specific information on the system except general conservation laws. In simple words, the maximum entropy method compares a measurement with our prior knowledge and extracts additional information from the observed discrepancies.

In the prior distribution, constrained only by the total energy conservation law, all isoenergetic product states are equally populated. In the actual distribution, energy randomization is expected to be as extensive as possible subject to the dynamical constraints that operate on the system. The maximum entropy analysis permits an identification of the dynamical constraints which preclude the distribution from being completely statistical.

We have investigated the bromine loss from vinyl bromide ions,

$$C_2H_3Br^+ \rightarrow C_2H_3^+ + Br, \tag{1}$$

which is by far the most important dissociation channel of this ion in the 10–20 eV photon energy range. This reaction has been studied by Miller and Baer with internal energy selection using threshold photoion–photoelectron coincidence spectroscopy (TPIPECO).[26] Based on scaling arguments, they concluded that the dissociation is statistical up to 2.1 eV above the threshold. In this paper we attempt to derive a quantitative measurement of the statistical character of the dissociation process by the maximum entropy method. In practice, we first measure the kinetic energy release distribution of the fragments resulting from dissociative ionization. This experimental distribution is then compared with the prior distribution and information concerning nonstatistical behavior is deduced. Particular attention is paid to the influence of the internal energy on the extent of ergodicity of phase space sampling.

II. EXPERIMENT

Three main approaches exist for obtaining the KERDs.

(i) Due to a large amplification factor, the metastable data obtained with a sector instrument provide good quality kinetic energy distributions, at least for not too large

[a)]Chercheur qualifié du F.N.R.S. (Belgium). Electronic mail: Bernard.Leyh@ulg.ac.be

releases, but with poor internal energy resolution.

(ii) The time-of-flight TPIPECO approach provides lower quality KERDs but with very good internal energy resolution so that it is best to restrict it to the determination of the first moment of the distribution as a function of internal energy E.

(iii) The approach followed in the present paper is somewhat intermediate. Its principle as well as its advantages and drawbacks are summarized in the next paragraphs.

The experimental setup has been designed for photoion–photoelectron coincidence measurements at fixed wavelength and is described in more detail elsewhere.[27] It consists of a Lindau-type electron energy analyzer and an ion retarding potential analyzer coupled with a quadrupole mass analyzer. The effusive gas sample is ionized by photons emitted from a rare gas discharge lamp. He(I) (at 21.21 eV), Ne(I) (at 16.67 and 16.85 eV), and Ar(II) (at 13.47 eV) resonance lines have been used for this study. Two kinds of spectra have been recorded.

(1) Ion kinetic energy spectra. The fragment ions are retarded within the chamber before mass selection. The true three-dimensional KERD is recovered from the experimental retarding potential curve in two steps: (i) the experimental ion kinetic energy spectrum is first fitted to an appropriate analytical form; (ii) the fitted function is differentiated and the derivative is multiplied by a correcting factor to take into account translational energy discrimination effects, as explained in Ref. 28. Using the energy and momentum conservation laws, the KERD of the fragment ion is then converted into the total KERD of both fragments.

As pointed out earlier,[28] the ion kinetic energy distribution obtained at this level is affected by the thermal kinetic energy distribution of the parent ion that contributes to broaden the ion KERD. However, for reaction (1), it has been checked that even for the less energetic dissociation [Ar(II) line], the influence of the parent thermal energy is almost negligible (less than 3.5% FWHM), so that no deconvolution is necessary.

(2) Photoelectron spectra. The single-photon ionization process is nonselective and leads to a broad distribution of internal energies of the parent ions. This distribution can be obtained by recording the appropriate photoelectron spectra. For a given dissociation channel, the internal energy distribution of parent ions giving rise to the fragments of interest, $D(E)$, is given by the photoelectron spectrum multiplied by the branching ratio of the fragments.[29] The branching ratio of the $[C_2H_3]^+$ ion has been calculated from TPIPECO data.[30] The measured KERD, denoted $\tilde{P}(\epsilon)$, is then given by

$$\tilde{P}(\epsilon)=\int_{\epsilon}^{\infty} D(E)P(\epsilon|E)dE, \tag{2}$$

where ϵ is the relative translational energy of the fragments and $P(\epsilon|E)$ is the KERD corresponding to a single internal energy E.

To summarize, internal energy is not resolved in the present approach. However, the internal energy distribution is known at a satisfactory level. The way the KERD is obtained is more direct and needs less assumptions than for time-of-flight TPIPECO data. Clearly, no ideal method exists, so that the best thing to do is to compare data obtained by complementary techniques.

We also studied reaction (1) in the metastable time window, observed in the first field-free region of a forward geometry sector mass spectrometer (AEI-MS9), by using the accelerating voltage scan technique[31] (V scan). Due to the very low value of the kinetic energy released in this dissociation, the influence of the parent ion thermal kinetic energy was taken into account to deconvolute the experimental V-scan spectrum. The KERD is obtained by differentiation of the deconvoluted spectrum after which the change of reference frame is taken into account.[32]

The C_2H_3Br sample gas (98% purity, inhibited with 200 ppm monoethyl ether hydroquinone) was provided by Aldrich Chemical Company Inc. and was used without further purification.

III. THE MAXIMUM ENTROPY METHOD

In the idealized case of a completely statistical dissociation, the probability of releasing a translational kinetic energy ϵ from a molecular ion having an excess internal energy E with respect to the dissociation asymptote is called the prior distribution, $P^0(\epsilon|E)$, and is given by the following formula:[1,23–25]

$$P^0(\epsilon|E)=C(E)\sqrt{\epsilon}N(E-\epsilon); \tag{3}$$

$C(E)$ is a normalization factor and $N(E\text{-}\epsilon)$ represents the vibrational–rotational energy level density of the pair of dissociating fragments, while $\sqrt{\epsilon}$ stands for the three-dimensional density of translational states.

Dynamical constraints prevent the actual KERD, $P(\epsilon|E)$, from being purely statistical. According to the maximum entropy principle, the observed distribution is that of the highest entropy among all those that satisfy the constraints.[12,13,15,33] This leads to

$$P(\epsilon|E)=P^0(\epsilon|E)\exp\left(-\lambda_0-\sum_{r=1}^{n}\lambda_r A_r\right), \tag{4}$$

where λ_0 and λ_r are Lagrange parameters and A_r are referred to as constraints or informative observables.

The entropy deficiency, DS, is defined as the difference between the entropy of the prior distribution S_0 and the entropy of the actual distribution S. It is given by

$$DS(E)=S_0-S=-\lambda_0-\sum_{r=1}^{n}\lambda_r\langle A_r\rangle. \tag{5}$$

The entropy deficiency gives access to the fraction of phase space actually sampled by the pair of fragments, de-

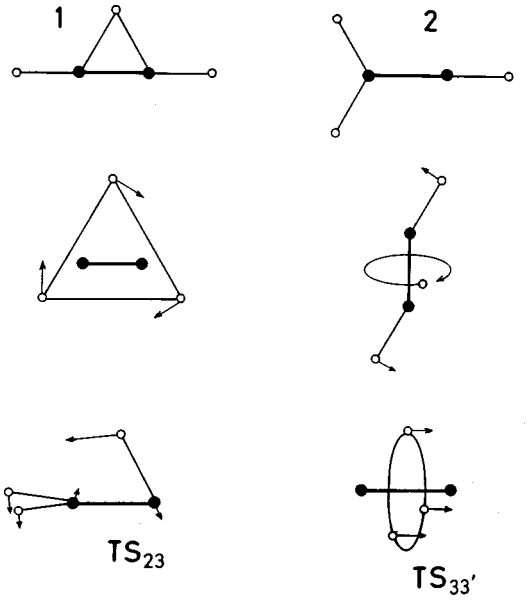

FIG. 1. Structures of the $C_2H_3^+$ ion. Top: most stable nonclassical bridged structure **1** and low-energy classical structure **2**. Middle part (left): dynamic structure, suggested by the spectroscopic analysis as an approximation to $\mathbf{TS_{12}}$; (right): dynamic structure suggested by Coulomb explosion imaging. Bottom: transition states $\mathbf{TS_{23}}$ and $\mathbf{TS_{33'}}$ detected in *ab initio* calculations and visualization of the large-amplitude motions associated with their imaginary modes.

noted F, which is given by the relationship $F=\exp(-DS)$.[34,35] For a purely statistical dissociation, $F=1$ (i.e., 100% phase space sampling).

As mentioned earlier, our experimental data involve an average over a range of internal energies of the parent ion. The observed KERD is then given, in its most general form, by substituting Eq. (4) into Eq. (2):

$$\tilde{P}(\epsilon)=\int_{\epsilon}^{\infty} D(E)P^0(\epsilon|E)\exp\left(-\lambda_0-\sum_{r=1}^{n}\lambda_r(E)A_r\right)dE. \quad (6)$$

IV. THE PRIOR DISTRIBUTION

The prior distribution $P^0(\epsilon|E)$ requires the calculation of the density of states of the $[C_2H_3]^+$ ion according to Eq. (3). What makes it a nontrivial exercise is that, at high energies, the $[C_2H_3]^+$ ion we are dealing with presents an unusually floppy structure or, more properly, a set of structures represented in Fig. 1.

Numerous reliable *ab initio* calculations[36,37] as well as a detailed spectroscopic analysis[38,39] have established that the minimum energy structure of the $C_2H_3^+$ ion corresponds to a nonclassical bridged structure belonging to the C_{2v} point group, which can be described as protonated acetylene, hereafter denoted structure **1**. The classical, Y-shaped, vinyl structure H_2CCH^+ (denoted **2**) is found to lie about 0.13 eV higher in energy and is now believed to be very close to a transition state (denoted $\mathbf{TS_{12}}$) in an internal rotation motion during which the three hydrogen atoms rotate as an equilateral triangle about a dumbell of two carbon atoms (Fig. 1). During this internal rotation, all of the nuclei remain in the same plane and there are six equivalent equilibrium conformations.[40,41]

TABLE I. Energies (in eV) of stationary points of $C_2H_3^+$ detected in *ab initio* calculations. See the text for the definition of the methods used.

Structure	Symmetry	Method A	Method B	Method C
1	C_{2v}	0	0	0
$\mathbf{2}\approx\mathbf{TS_{12}}$	C_{2v}/C_s	0.03	0.14	0.12
3	C_{3v}	2.06	2.03	2.00
$\mathbf{TS_{23}}$	C_s	2.14	2.10	2.08
$\mathbf{TS_{33'}}$	D_{3h}	4.58	4.52	4.52

The Coulomb explosion imaging method[42] confirms the picture of a highly fluxional dynamical system,[43] but suggests that one of the hydrogen atoms undergoes a circular orbit around an acetylene core[44] (Fig. 1).

Dynamical *ab initio* calculations have emphasized the fact that the nature of the large-amplitude motions carried out by the hydrogen atoms depends on the available internal energy.[45,46] The vibrational quantum ground state of $C_2H_3^+$ corresponds indeed to the planar nonclassical bridged structure **1**. However, at higher internal energies, a broad distribution of nonplanar structures is observed. This result suggests that the Coulomb explosion experiments ''probes an ensemble of rovibrationally excited'' ions.[46]

In an attempt to investigate the situation in more detail, a series of *ab initio* calculations have been carried out. They revealed the existence of an additional minimum of the potential energy surface, hereafter denoted **3**, corresponding to the H_3CC^+ structure and belonging to the C_{3v} point group. Furthermore, isomers **2** and **3** are found to be connected by a transition state $\mathbf{TS_{23}}$, whereas **3** and the equivalent CCH_3^+ structure **3′** are connected by a third transition state $\mathbf{TS_{33'}}$. Both are represented in Fig. 1. In order to check the stability of the predictions, calculations have been carried out with the GAUSSIAN system of programs[47] at nine levels of accuracy. Only the three best ones are reported here. Using the usual conventions,[48] they are described by the following acronyms:

(A) B3LYP/cc-pVTZ (102 basis functions);

(B) QCISD/6-311++G(3df,2pd)//QCISD/6-311+G(d,p) (123 basis functions);

(C) QCISD/aug-cc-pVTZ//QCISD/aug-cc-pVDZ (161 basis functions).

The relative energy of the various stationary points, including zero-point energy corrections, is reported in Table I. The independence of the results from the nature of the basis set and from the way the correlation energy is calculated is remarkable, except for the relative energy of structures **1** and **2**, which is known to require a very elaborate treatment of the correlation energy.

It should be noted that each transition state structure indicates the onset of a regime where a CH bending mode is replaced by a large-amplitude motion.

According to the recommendations of Scott and Radom,[49] the vibrational modes of all of the stationary points have been calculated at the B3LYP/6-31G(d) level and afterward scaled by a factor of 0.9806. Those of the lowest-energy structure **1** will now be reviewed.

(1) $Q_1(b_2)$ is the ring deformation at 350 cm^{-1}. Above 0.12

eV, it transforms into an in-plane internal rotor having a rotational constant of 4 cm^{-1} and a symmetry number equal to 6. This mode, represented in Fig. 1, has been extensively studied by Escribano and Bunker[40] and by Hougen.[41]

(2) $Q_2(a_2)$ is the out-of-plane CH antisymmetric bend at 587 cm^{-1}. Above 2.1 eV, it is assumed to transform into an out-of-plane internal rotor having a rotational constant of 6 cm^{-1} and a symmetry number equal to 3. This transformation takes place via transition state $\mathbf{TS_{23}}$, represented in Fig. 1.

(3) $Q_3(b_1)$ is the out-of-plane CH symmetric bend at 781 cm^{-1}. Above 4.5 eV, it transforms into a back-and-forth motion of an H_3 ring encircling the CC axis. The amplitude is large and takes place over the barrier of a double minimum potential. The corresponding transition state is denoted $\mathbf{TS_{33'}}$ and is represented in Fig. 1.

(4) $Q_4(a_1)$ is the in-plane CH symmetric bend at 889 cm^{-1}.

(5) $Q_5(b_2)$ is the in-plane CH antisymmetric bend at 1173 cm^{-1}.

(6) $Q_6(a_1)$ is the CC stretch at 1925 cm^{-1}.

(7) $Q_7(a_1)$ is the symmetric stretch (at 2268 cm^{-1}) between the bridging hydrogen and a heavy acetylene framework. The reaction coordinate of the lowest dissociation path $C_2H_3^+ \rightarrow C_2H_2^+ + H$ ($D_e = 4.39$ eV) has a major component on this mode.

(8) $Q_8(b_2)$ is the CH antisymmetric stretch. It has been observed[38] as a fundamental vibration at 3142 cm^{-1} (whereas the calculated value is 3173 cm^{-1}).

(9) $Q_9(a_1)$ is the in plane CH symmetric stretch at 3279 cm^{-1}.

The calculated rotational constants agree very well with the observed values. One has $B_y = 13.34\,cm^{-1}$, $B_z = 1.14\,cm^{-1}$, and $B_x = 1.05\,cm^{-1}$, z being the symmetry axis and y being parallel to the CC axis. The rotation around z has a symmetry number equal to 2.

The rovibrational density of states of the $C_2H_3^+$ ion has been calculated by the Beyer–Swinehart algorithm.[1,50,51] The anharmonicity of Q_7 has been taken into account. The algorithm has been extended to allow Q_1, Q_2, and Q_3 to change their nature above a certain critical energy, as described above.

However, even with these improvements, the reliability of such a calculation can be questioned when the internal energy of the $C_2H_3^+$ ion is as large as 8 eV, as in some of the experiments reported in this paper. Then, the hydrogen atoms are no longer localized to regions near an equilibrium configuration but undergo exceedingly large-amplitude motions. Therefore, to simulate such a highly fluxional system, the calculation of the energy-level density has been carried out in an alternative way. The CH bonds are described as three three-dimensional oscillators with cylindrical symmetry.[52] Thus, the model consists of one harmonic CC bond (identical with Q_6 above), three anharmonic CH stretching modes having a frequency of 2896 cm^{-1} (an average value of Q_7, Q_8, and Q_9) and a dissociation limit at 4.39 eV, six anharmonic CH bending modes having a frequency of 624 cm^{-1} (an average value of Q_1 to Q_5 plus B_y)

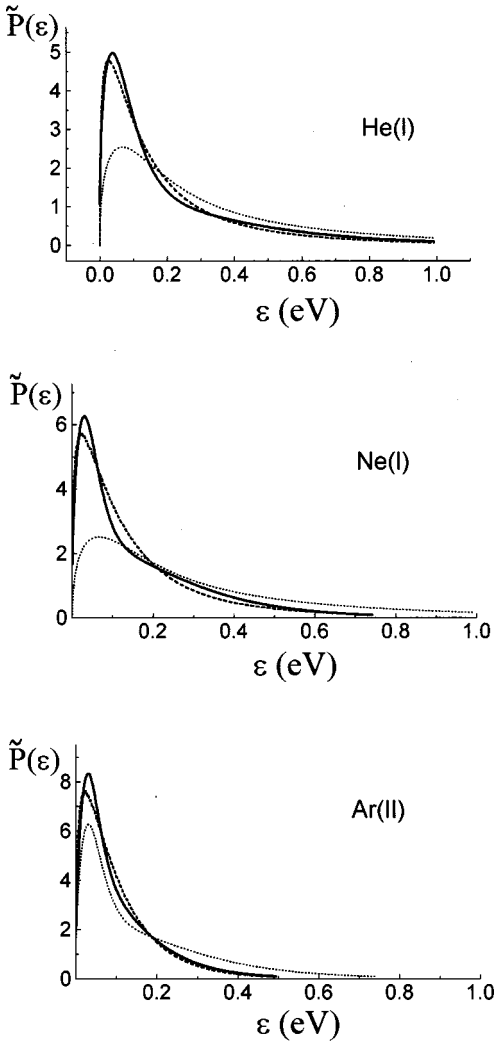

FIG. 2. Kinetic energy release distributions, $\tilde{P}(\epsilon)$ (in eV^{-1}), obtained for the $C_2H_3Br^+ \rightarrow [C_2H_3]^+ + Br$ dissociation with He(I), Ne(I), and Ar(II) resonance lines. Solid line: experimental; dashed line: least-squares fit to the functional form given by Eq. (7); dotted line: prior KERD averaged over the internal energy distribution.

and converging to a limit at 4.5 eV (at which the three hydrogens scramble freely). The two overall rotations about axes x and z are added to this set. It is gratifying to note that, at an internal energy as high as 8.5 eV, the energy-level densities calculated by the two methods differ by less than a factor of 2.

The other fragment, the bromine atom, can be formed either in the $^2P_{1/2}$ or the $^2P_{3/2}$ spin–orbit levels, which are separated by 0.45 eV. Both were included in our calculation of the prior distribution, with their respective statistical weights.

V. RESULTS

A. One-photon dissociative ionization

Figure 2 represents the experimental KERDs obtained with the three available resonance lines. Their average kinetic energies are given in Table II. Figure 2 also displays the prior distribution averaged over the sampled domain of internal energy. The discrepancies with respect to the experi-

TABLE II. Average excess internal energies and average kinetic energy releases observed with different resonance lines.

Resonance line	$\langle E_{\text{excess}} \rangle$ (eV)	$\langle \epsilon \rangle$ (eV)
He(I)	3.15	0.132
Ne(I)	2.49	0.109
Ar(II)	0.76	0.073

mental data indicate the occurrence of nonstatistical effects. Therefore a maximum entropy analysis was attempted.

All distributions are expected to be accounted for by the use of a single constraint since they are broad and do not show any fine structure. Actually, as can be seen in Fig. 2, the experimental KERDs can be reasonably well fitted to the following equation, using a least-squares algorithm:

$$\tilde{P}(\epsilon) = \int_{\epsilon}^{\infty} D(E) P^0(\epsilon|E) \exp(-\lambda_0) \exp[-\lambda_1(E)\sqrt{\epsilon}] dE, \tag{7}$$

where the value of the Lagrange multiplier λ_1 is energy dependent.

In order to achieve a satisfactory fit of the experimental KERDs and due to the broad range of internal energies sampled in some of the experiments, it was necessary to take the variation of λ_1 with energy into account. A Gaussian dependence,

$$\lambda_1(E) = a_1 \exp\left[-\left(\frac{E}{a_2}\right)^2\right], \tag{8}$$

was found to be appropriate. From Fig. 3 it is clearly seen that with increasing energy the constraint becomes less effective and drops to near zero at very high internal energies.

The fit is somewhat worse for the KERD obtained with the Ne(I) resonance line than for He(I) and Ar(II). However, we found no other constraint that gave a better fit. A competitive dissociation mechanism involving an autoionizing state situated at 16.85 eV and observed by absorption spectroscopy[53] can be invoked in that case. This energy is resonant with one of the components of the Ne(I) doublet resonance line and the consequences of such a situation will be analyzed in a forthcoming publication.[53] Nevertheless, even in this case, the agreement is sufficiently good to conclude that direct ionization is the dominant mechanism. The KERD determined with the Ar(II) line is closer to the averaged prior distribution (Fig. 2) than in the other two cases. This results from the fact that, when the internal energy is low, the average value of $\lambda_1 \epsilon^{1/2}$ is very small and the influence of the constraint is almost negligible.

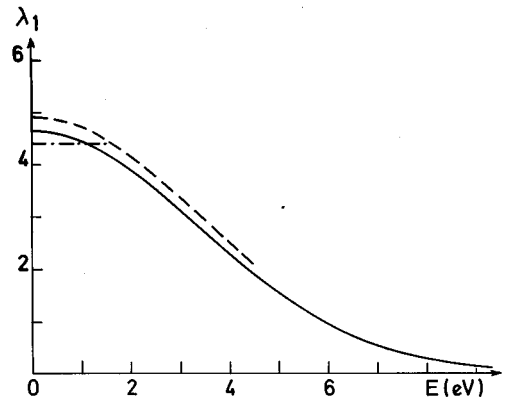

FIG. 3. Variation of the Lagrange parameter λ_1 (in $eV^{-1/2}$) with excess internal energy E derived from the KERDs measured with the three resonance lines: He(I) (solid line), Ne(I) (dashed), and Ar(II) (dashed–dotted line).

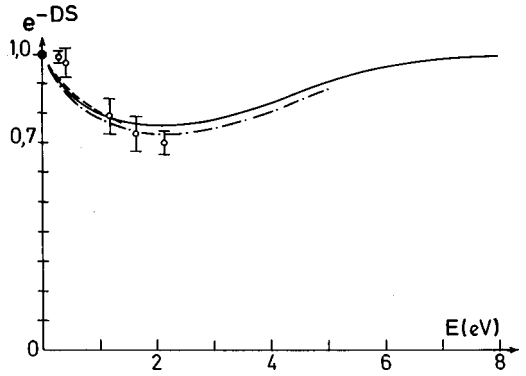

FIG. 4. Efficiency of phase space sampling $\exp(-DS)$ as a function of excess internal energy E. Curves: excitation resulting from various resonance lines: He(I) (solid line), Ne(I) (dashed–dotted line) and Ar(II) (dashed). Open symbols with error bars: values of $\exp(-DS)$ derived from TPIPECO experiments of Miller and Baer (Ref. 26). The dot at $E=0$ results from the analysis of the metastable transition (this work).

On the whole, the data contained in Fig. 2 can be accounted for by a single constraint, viz. $\epsilon^{1/2}$. This observation has to be related to the ''momentum gap law,'' [54,55] which has been suggested to control the vibrational predissociation dynamics of halogenobenzene and pyridine ions.[24,25] The effect of this constraint is that states with large translational energy are disfavored and the energy in excess with respect to the dissociation asymptote is preferentially channeled into rovibrational energy of the fragments.

The main result of the present article is given in Fig. 4, which shows the fraction of phase space sampled as a function of internal energy. It is obvious that, while for low and high internal energies the allowed phase space is almost completely sampled, at intermediate energies the accessible portion is reduced. In that range, the situation is not purely ergodic. However, a 75% efficiency is still reached and the dissociation can be considered to be nearly statistical. Similar efficiencies were observed in the metastable window for the halogenobenzene and pyridine cations.[23–25]

The quality of the various fits performed is not as good as that previously obtained in the analysis of metastable dissociations.[23–25] This is certainly related to the width of the energy range sampled in the present experiments. However, we do not draw any conclusion from isolated data but only from the comparison of three independent sets of data obtained with different resonance lines and corresponding therefore to different internal energy contents. The quite good overlap between the results deduced from these three experiments pleads in favor of the reliability of the method. In addition, as now shown in the next paragraph, our data are in very good agreement with those of Miller and Baer[26] in the energy domain investigated by these authors.

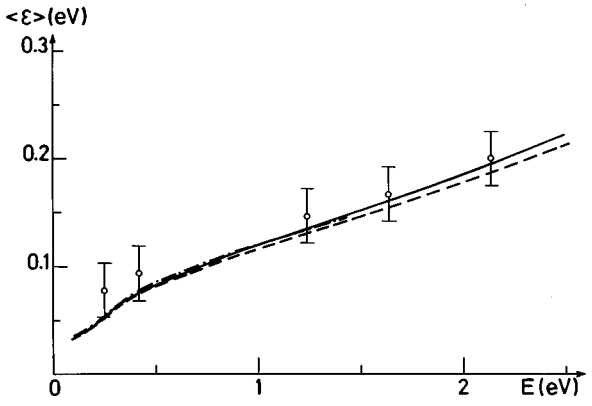

FIG. 5. Average kinetic energy release as a function of excess energy. The open symbols with error bars are taken from Ref. 26. The lines are calculated according to Eq. (10) with λ_1 values obtained from, respectively, He(I) (solid line), Ne(I) (dashed), and Ar(II) (dashed–dotted line) data.

B. Internal energy-resolved average kinetic energy releases

In the framework of the maximum entropy method, the knowledge of the constraints and of the Lagrange parameters is sufficient to completely define the experimental KERD. Having determined the unique constraint and the variation of the $\lambda_1(E)$ parameter with internal energy, we are now able to recover internal energy-resolved data. At each particular energy, the KERD that should have been observed in an energy-resolved experiment (typically PIPECO[9]) can simply be calculated by:

$$P(\epsilon|E)=\frac{\sqrt{\epsilon}N(E-\epsilon)\exp[-\lambda_0-\lambda_1(E)\sqrt{\epsilon}]}{\int_0^E\sqrt{\epsilon}N(E-\epsilon)\exp[-\lambda_0-\lambda_1(E)\sqrt{\epsilon}]d\epsilon}. \quad (9)$$

The average kinetic energy releases calculated by

$$\langle\epsilon\rangle=\int_0^E\epsilon P(\epsilon|E)d\epsilon \quad (10)$$

are plotted as a function of the excess energy E in Fig. 5. The three curves are calculated independently using λ_1 values extracted from the analysis of the He(I), Ne(I), and Ar(II) data, respectively. They are in very good agreement with each other as well as with the TPIPECO values of Miller and Baer.[26]

As an alternative, the reverse procedure is also possible. The value of λ_1 (and hence of e^{-DS}) can be obtained by fitting to Eq. (10) the values of $\langle\epsilon\rangle$ determined by Miller and Baer in their energy-resolved measurements.[26] The results are reported in Fig. 4. At an internal energy $E=0.28$ eV, we find $e^{-DS}=0.99$. The efficiency of phase space sampling then decreases regularly as a function of E and reaches a value of about 70% when $E=2.13$ eV. An excellent agreement is observed between these discrete data and the curves derived from the maximum entropy analysis of our own KERDs.

C. The metastable transition

The point at nearly zero excess internal energy in Fig. 4 results from a study of reaction (1) in the metastable time range sampled in a tandem mass spectrometer. The fraction of phase space has been calculated by relating the value of e^{-DS} to the position and the value of the maximum of the KERD using a general method reported elsewhere.[56] The metastable dissociation is characterized by an unknown range of internal energies. In the present case, however, the average kinetic energy released is extremely low (0.002 eV), so that it can be argued that the metastable dissociation occurs very close to the threshold with a very narrow internal energy distribution. From the calculation of the metastable transmission function,[57] the rate constant at the most probable internal energy is equal to $3.5\times10^5\,s^{-1}$. A RRKM rate constant calculation at threshold including the external rotor around the reaction axis leads to $k(E_0)=1/hN(E_0)=7.5\times10^4\,s^{-1}$ and supports the idea that the time window accessible in this experiment (2.1–3.8 μs) samples the threshold energy region.

VI. DISCUSSION

The quantity e^{-DS} measures the degree of phase space sampling (or ''exploration'')[34,35] with respect to the uniform situation postulated by statistical theories of unimolecular reactivity. Two questions arise now. First, how is the maximum entropy method related to alternative approaches for analyzing the KERDs? Second, does e^{-DS} really measure the efficiency of intramolecular vibrational redistribution (IVR) among a set of oscillators?

A. Comparison with Klots' theory

Following Klots,[1,3,58,59] many authors have parametrized KERDs by the empirical equation

$$P(\epsilon)\div\epsilon^n\exp(-\alpha\epsilon), \quad (11)$$

where the exponent n is assumed to vary between 0 and 1. A value of n close to zero generates a two-dimensional (2-D) Boltzmann distribution. This has been found, e.g., in the dissociation of methyl iodide ions.[1,60,61] Values of n close to 1 generate 4-D distributions, which are expected to be suitable for H-atom loss reactions.[1] However, in the case of loosely bound systems, Lifshitz has consistently found values close to 0.5.[62–65]

Note that the maximum of the distribution (11) takes place at $\epsilon_M=n/\alpha$. An alternative to Eq. (11) could be $\epsilon^n(1-\epsilon/E)^s$ whose maximum falls at $\epsilon_M=nE/(s+n)$.

In the maximum entropy method, the KERDs would be parametrized as, e.g., $\epsilon^{1/2}\exp(-\lambda_1\epsilon^{1/2})\exp(-\alpha\epsilon)$, which admits its maximum at $\epsilon_M\approx(1/2\alpha)(1-\lambda_1/\sqrt{2\alpha})$, or, alternatively, as $\epsilon^{1/2}\exp(-\lambda_1\epsilon^{1/2})(1-\epsilon/E)^S$, which admits its maximum at $\epsilon_M\approx E/(2s+1)-\lambda_1[E/(2s+1)]^{3/2}+\cdots$.

Therefore, the value $n=0.5$ (3-D distribution) is seen to correspond to the fully statistical prior distribution ($\lambda_1=0$). This implies that weak constraints, if any, operate on cluster evaporation. By contrast, KERDs closer to a 2-D distribution are usually ascribed to strong interactions between separating fragments. In the maximum entropy language, they indicate a constrained situation described by a positive value of the Lagrange multiplier λ_1.

B. Mechanism of phase space sampling

We are faced with an apparent contradiction. On the one hand, e^{-DS} is found to increase and to tend to one as the internal energy E approaches 8 eV. On the other hand, at such a high value of the internal energy, the lifetime is expected to be very short and thus to leave little time for a purely vibrational mechanism.

We interpret this by proposing that, at least for high values of E, energy randomization does not exclusively depend on the coupling among vibrational modes brought about by the anharmonicity of the potential energy surface of the ground state of the molecular ion. It also results from fast radiationless transitions among potential energy surfaces. Internal conversions are known to proceed from conical intersections with very large rate constants ($\approx 10^{13}\,s^{-1}$)[66] and these intersections are recognized as a source of chaos in the dynamics. Well-studied examples have been found in open-shell systems like NO_2 or $C_2H_4^+$, whose extremely irregular spectra are now interpreted as paradigms of molecular chaos.[67–70] As the energy increases, the seams between the crossing surfaces are expected to extend over larger portions of configuration space, thereby providing a wide variety of initial conditions for the trajectories in phase space. Thus, just as in the case of thermal reactions, energy randomization is greatly facilitated by the fact that the initial conditions are already scattered all over phase space.[11,71,72] Since, in addition, the efficiency of anharmonic coupling increases with E, a nearly uniform distribution of trajectories in phase space can be achieved at high internal energies, even if the lifetime is very short.

Nonadiabatic interactions and, in particular, conical intersections are expected to occur more frequently in the case of ionized molecules than for neutrals (because of higher densities of states) and to generate stronger vibronic coupling (because the off-diagonal elements are larger in open-shell system).[73,74] This may account for the fact that statistical theories of unimolecular reactions are found to work extremely well in the case of ions. Therefore, mode selective chemistry is presumably not to be expected in the case of ionized species, unless excitation processes much more selective than electron-impact or single-photon ionization are used.

VII. SUMMARY AND CONCLUDING REMARKS

The main conclusions of this article can be summarized as follows.

(1) The $C_2H_3^+$ ion is a much more floppy species than commonly thought. As the internal energy increases, several vibrational modes are successively transformed to large-amplitude motions.
(2) What has been attempted here is to extract energy-resolved data from dissociative ionization and to compare them with the TPIPECO data of Miller and Baer[26] as well as with a study of the metastable dissociation. The maximum entropy method unifies the results obtained by these different experimental techniques and provides a convincing overall picture.
(3) A single constraint is sufficient to account for the shape of the KERDs obtained for the dissociations of ions characterized by different internal energy ranges. The functional form of the constraint, $\epsilon^{1/2}$, is related to the momentum gap law.[54,55] High translational energy release is disfavored, while energy channeling into rotational and vibrational degrees of freedom is favored with respect to a purely statistical partitioning.
(4) The analysis provides us with the evolution of the entropy deficiency and hence the fraction of phase space sampled as a function of excess internal energy. The important point is that the constraint is less effective both at very low and at very high internal energies, while at intermediate energies it reduces to nearly 75% the fraction of phase space available to the fragments. The almost complete phase space sampling at high internal energies is believed to be due not only to the internal vibrational relaxation but also to fast internal conversions that generate chaos.

ACKNOWLEDGMENTS

JCL is indebted to Professor R. D. Levine for suggesting the use of three-dimensional oscillators in the calculation of high-energy densities of states. AH is grateful to Dr. F. Remacle and Dr. P. Urbain for many useful discussions and their help concerning the least-squares fit programs. This work has been supported by the ''Actions de Recherche Concertée (ARC)'' (Direction de la Recherche Scientifique—Communauté Française de Belgique). BL is indebted to the F.N.R.S. (Belgium) for a research associate position.

APPENDIX: DENSITY OF STATES OF A FLUXIONAL MOLECULE

Contrary to what might have been expected, there is no sudden increase of the density of states when one degree of freedom suddenly switches from an oscillator to a rotor quantization above a certain critical energy E_1.

Consider the convolution between a first subsystem, denoted the bath, whose density of states is assumed to increase exponentially with its internal energy,

$$N_1(E) = C \exp(\alpha E).$$

The second subsystem behaves as a harmonic oscillator below E_1,

$$N_2(E) = \sum_{j=0} \delta(E - h\nu_j), \quad E < E_1,$$

and as a rigid rotor above that energy,

$$N_2(E) = (\sigma \sqrt{E - E_1}\sqrt{B})^{-1}, \quad E > E_1.$$

The overall density of states, denoted $N_{\mathrm{conv}}(E)$ is obtained by convoluting the two subsystems:

$$N_{\mathrm{conv}}(E)=\int_0^E N_1(E-x)N_2(x)dx$$

$$=Ce^{\alpha E}\sum_{j=0}\int_0^{E_1} e^{-\alpha x}\delta(x-h\nu_j)dx$$

$$+Ce^{\alpha E}\frac{1}{\sigma\sqrt{B}}\int_{E_1}^{E}\frac{e^{-\alpha x}}{\sqrt{x-E_1}}dx$$

$$=N_1(E)(1-e^{-\alpha h\nu})^{-1}+\frac{\sqrt{\pi}}{\sigma\sqrt{B}\sqrt{\alpha}}N_1(E-E_1)$$

$$\times\mathrm{erf}[\sqrt{\alpha(E-E_1)}].$$

Compare this result with the situation that would obtain if the oscillator remained harmonic at all energies:

$$N_{\mathrm{har}}(E)=N_1(E)(1-e^{-\alpha h\nu})^{-1}.$$

The increase in the density of states brought about by the change in the nature of the second subsystem is negligible at internal energies E close to E_1, especially if E_1 is large:

$$\frac{N_{\mathrm{conv}}(E)-N_{\mathrm{har}}(E)}{N_{\mathrm{har}}(E)}=\left(\frac{2}{\sigma}\right)(1-e^{-\alpha h\nu})\sqrt{\frac{E-E_1}{B}}e^{-\alpha E_1}$$

$$[\text{low values of } (E-E_1)]$$

$$=\frac{\sqrt{\pi}}{\sigma\sqrt{B}\sqrt{\alpha}}(1-e^{-\alpha h\nu})e^{-\alpha E_1}$$

$$[\text{high values of } (E-E_1)].$$

A similar result is obtained if $N_1(E)$ is parametrized as CE^S.

[1] T. Baer and W. L. Hase, *Unimolecular Reaction Dynamics. Theory and Experiments* (Oxford University Press, New York, 1996).
[2] C. E. Klots, J. Chem. Phys. **58**, 5364 (1973).
[3] C. E. Klots, J. Chem. Phys. **64**, 4269 (1976).
[4] C. Lifshitz, Adv. Mass Spectrom. **7A**, 3 (1978).
[5] C. Lifshitz, J. Phys. Chem. **87**, 2304 (1983).
[6] C. Lifshitz, Adv. Mass Spectrom. **12**, 315 (1992).
[7] W. J. Chesnavich and M. T. Bowers, in *Gas Phase Ion Chemistry*, edited by M. T. Bowers (Academic, New York, 1979).
[8] P. J. Derrick and K. F. Donchi, in *Comprehensive Chemical Kinetics*, edited by C. H. Bamford and C. F. H. Tipper (Elsevier, Amsterdam, 1983), Vol. 24.
[9] T. Baer, Adv. Chem. Phys. **64**, 111 (1986).
[10] I. Powis, Acc. Chem. Res. **20**, 179 (1987).
[11] J. C. Lorquet, Mass Spectrom. Rev. **13**, 233 (1994).
[12] R. D. Levine and R. B. Bernstein, in *Dynamics of Molecular Collisions*, edited by W. H. Miller (Plenum, New York, 1976), Part B.
[13] R. D. Levine and J. L. Kinsey, in *Atom–Molecule Collision Theory. A Guide for the Experimentalist*, edited by R. B. Bernstein (Plenum, New York, 1979).
[14] R. D. Levine, Adv. Chem. Phys. **47**, 239 (1981).
[15] R. D. Levine, in *Theory of Chemical Reaction Dynamics*, edited by M. Baer (CRC, Boca Raton, FL, 1985).
[16] J. Momigny, R. Locht, and G. Caprace, Int. J. Mass Spectrom. Ion Processes **71**, 159 (1986).
[17] J. Momigny, R. Locht, and G. Caprace, Chem. Phys. **102**, 275 (1986).
[18] J. Momigny and R. Locht, Chem. Phys. Lett. **211**, 161 (1993).
[19] J. Momigny and R. Locht, Chem. Phys. **206**, 225 (1996).
[20] C. Lifshitz and E. Tzidony, Int. J. Mass Spectrom. Ion Phys. **39**, 181 (1981).
[21] C. Lifshitz, Int. J. Mass Spectrom. Ion Phys. **43**, 179 (1982).
[22] Y. S. Cho, J. C. Choe, and M. S. Kim, J. Phys. Chem. **99**, 8645 (1995).
[23] P. Urbain, F. Remacle, B. Leyh, and J. C. Lorquet, J. Phys. Chem. **100**, 8003 (1996).
[24] P. Urbain, B. Leyh, F. Remacle, A. J. Lorquet, R. Flammang, and J. C. Lorquet, J. Chem. Phys. **110**, 2911 (1999).
[25] P. Urbain, B. Leyh, F. Remacle, and J. C. Lorquet, Int. J. Mass Spectrom. **185/186/187**, 155 (1999).
[26] B. E. Miller and T. Baer, Chem. Phys. **85**, 39 (1984).
[27] R. Locht and C. Servais, Z. Phys. Chem. (Munich) **195**, 153 (1996).
[28] A. Hoxha, B. Leyh, and R. Locht, Rapid Commun. Mass Spectrom. **13**, 275 (1999).
[29] T. Baer and P. M. Mayer, J. Am. Soc. Mass Spectrom. **8**, 103 (1997).
[30] A. Hoxha, B. Leyh, R. Locht, M. Malow, K. M. Weitzel, and H. Baumgärtel, Bessy Jahresbericht **1998**, 178.
[31] K. R. Jennings, J. Chem. Phys. **43**, 4176 (1965).
[32] J. L. Holmes, A. D. Osborne, and G. Weese, Int. J. Mass Spectrom. Ion Phys. **19**, 207 (1976).
[33] R. D. Levine and R. B. Bernstein, *Molecular Reaction Dynamics and Chemical Reactivity* (Oxford University Press, New York, 1987).
[34] F. Iachello and R. D. Levine, Europhys. Lett. **4**, 389 (1987).
[35] R. D. Levine, Adv. Chem. Phys. **70**, 53 (1988).
[36] L. A. Curtiss and J. A. Pople, J. Chem. Phys. **88**, 7405 (1988).
[37] R. Lindh, J. E. Rice, and T. J. Lee, J. Chem. Phys. **94**, 8008 (1991).
[38] M. W. Crofton, M. F. Jagod, B. D. Rehfuss, and T. Oka, J. Chem. Phys. **91**, 5139 (1989).
[39] C. M. Gabrys, D. Uy, M. F. Jagod, T. Oka, and T. Amano, J. Phys. Chem. **99**, 15611 (1995).
[40] R. Escribano and P. R. Bunker, J. Mol. Spectrosc. **122**, 325 (1987).
[41] J. T. Hougen, J. Mol. Spectrosc. **123**, 197 (1987).
[42] Z. Vager, R. Naaman, and E. P. Kanter, Science **244**, 426 (1989).
[43] E. P. Kanter, Z. Vager, G. Both, and D. Zajfman, J. Chem. Phys. **85**, 7487 (1986).
[44] Z. Vager, D. Zajfman, T. Graber, and E. P. Kanter, Phys. Rev. Lett. **71**, 4319 (1993).
[45] J. S. Tse, D. D. Klug, and K. Laasonen, Phys. Rev. Lett. **74**, 876 (1995).
[46] D. Marx and M. Parrinello, Science **271**, 179 (1996).
[47] M. J. Frisch, G. W. Trucks, H. B. Schlegel, *et al.*, GAUSSIAN 94 (Revision B.3) (Gaussian Inc., Pittsburgh, 1995).
[48] W. J. Hehre, L. Radom, P. von Rague Schleyer, and J. A. Pople, *Ab Initio Molecular Orbital Theory* (Wiley, New York, 1986).
[49] A. P. Scott and L. Radom, J. Phys. Chem. **100**, 16 502 (1996).
[50] S. E. Stein and B. S. Rabinovitch, J. Chem. Phys. **58**, 2438 (1973).
[51] R. G. Gilbert and S. C. Smith, *Theory of Unimolecular and Recombination Reactions* (Blackwell Scientific, Oxford, 1990).
[52] L. Pauling and E. B. Wilson, *Introduction to Quantum Mechanics* (McGraw-Hill, New York, 1935).
[53] A. Hoxha, R. Locht, B. Leyh, H. W. Jochims, and H. Baumgärtel (in preparation).
[54] G. E. Ewing, J. Chem. Phys. **71**, 3143 (1979).
[55] G. E. Ewing, J. Chem. Phys. **72**, 2096 (1980).
[56] J. C. Lorquet, Int. J. Mass Spectrom. (submitted).
[57] J. L. Holmes and J. K. Terlouw, Org. Mass Spectrom. **15**, 383 (1980).
[58] C. E. Klots, Acc. Chem. Res. **21**, 16 (1988).
[59] C. E. Klots, Z. Phys. D **20**, 105 (1991).
[60] D. M. Mintz and T. Baer, J. Chem. Phys. **65**, 2407 (1976).
[61] I. Powis, Chem. Phys. **74**, 421 (1983).
[62] C. Lifshitz, P. Sandler, H.-F. Grützmacher, J. Sun, T. Weiske, and H. Schwarz, J. Phys. Chem. **97**, 6592 (1993).
[63] W. Y. Feng and C. Lifshitz, J. Phys. Chem. **98**, 6075 (1994).
[64] W. Y. Feng, V. Aviyente, T. Varnali, and C. Lifshitz, J. Phys. Chem. **99**, 1776 (1995).
[65] C. Lifshitz and W. Y. Feng, Int. J. Mass Spectrom. Ion Processes **146/147**, 223 (1995).
[66] H. Köppel, W. Domcke, and L. S. Cederbaum, Adv. Chem. Phys. **57**, 59 (1984).
[67] D. M. Leitner, H. Köppel, and L. S. Cederbaum, J. Chem. Phys. **104**, 434 (1996).
[68] E. Leonardi, C. Petrongolo, G. Hirsch, and R. J. Buenker, J. Chem. Phys. **105**, 9051 (1996).
[69] F. Santoro, J. Chem. Phys. **109**, 1824 (1998).
[70] R. F. Salzgeber, V. A. Mandelshtam, C. Schlier, and H. S. Taylor, J. Chem. Phys. **110**, 3756 (1999).
[71] S. Nordholm and S. A. Rice, J. Chem. Phys. **62**, 157 (1975).
[72] F. Remacle and R. D. Levine, J. Phys. Chem. **95**, 7124 (1991).
[73] J. C. Lorquet, in *The Structure, Energetics and Dynamics of Organic Ions*, edited by T. Baer, C. Y. Ng, and I. Powis (Wiley, Chichester, 1996).
[74] H. Köppel, Chem. Phys. **77**, 359 (1983).